

ESTIMATION OF DIELECTRIC LOSSES IN THE BESSY VSR WARM BEAM PIPE ABSORBERS*

T. Flisgen[†], H.-W. Glock, and A. Tsakanian

Helmholtz-Zentrum Berlin für Materialien und Energie GmbH (HZB), 12489 Berlin, Germany

Abstract

Currently Helmholtz-Zentrum Berlin prepares the update of the BESSY II ring to BESSY VSR. The updated ring will be capable of simultaneously storing short and long bunches to satisfy the various user demands. For this sake, a cryomodule accommodating two 1.5 GHz and two 1.75 GHz superconducting cavities will be installed into the storage ring. The cavity string will be equipped with warm dielectric absorber rings at both ends. Together with the waveguide dampers of the cavities, these rings damp electromagnetic fields excited by the beam. This contribution presents the estimation of the dielectric losses in the beam pipe absorber rings of the BESSY VSR module. The presented approach is based on determining a broad band impedance of the dielectric ring by exciting the numerical model with a single broad band Gaussian bunch. Subsequently, the power deposited into the ring is estimated in the frequency domain by multiplying the impedance with the square of the beam current for all considered harmonics of the beam. Finally, these power contributions are added up. In addition to details of the scheme, the contribution presents results for the recent absorber layout of the BESSY VSR string.

INTRODUCTION

BESSY II is a third generation light source located at the Wilhelm-Conrad-Röntgen Campus in Berlin Adlershof in Germany. It serves as user facility for various experiments with photon pulses ranging from the Terahertz to the hard X-ray regime. The main ring of the facility has a circumference of 240 m and is able to store currents up to 300 mA with an energy of 1.7 GeV. Depending on the requests of the users, the machine can be operated in various modes. Currently, the upgrade of the ring to BESSY VSR (Variable pulse-length Storage Ring) is planned to allow for simultaneously storing long and short pulses in the machine [1–4]. For this sake, a cryomodule (see Figure 2 in [3]) accommodating two superconducting 1.5 GHz and two superconducting 1.75 GHz four-cell resonators will be installed into the storage ring. The superposition of the accelerating voltages from the four cavities results in a beating pattern of the voltage: Every second bunch, the derivative of the voltage cancels, whereas for the remaining bunches the derivative of the voltage constructively adds up. In combination with the machine optics, the voltage beating pattern leads to long and short pulses simultaneously stored in the machine.

* The research leading to these results was supported by the German Bundesministerium für Bildung und Forschung, Land Berlin and grants of Helmholtz Association.

[†] thomas.flisgen@helmholtz-berlin.de

As depicted in Figure 2 in [3], each of the four cavities in the VSR cryomodule is equipped with three waveguide absorbers to lower the quality factors of higher-order modes in the cavities. In addition, two warm beam-pipe loads (refer to Figure 3 in [3]) are attached to both ends of the cavity string to avoid propagation of energy into the BESSY ring and reflection of energy into the module. These warm loads will be made of silicon carbide (SC-35) and will have a length of 120 mm, an inner radius of 55 mm, and an outer radius of 70 mm. The aim of this paper is the numerical estimation of power deposited by the BESSY VSR beam (see Figure 2.5 in [2] for the bunch filling pattern with long and short pulses) into the warm absorber rings. First, the theory of the dielectric loss computation is discussed, subsequently the results of the numerical calculations are presented, and finally the conclusions and the outlook are given.

THEORY OF DIELECTRIC LOSS COMPUTATION

The dielectric losses in the warm absorbers are determined according to Poynting's theorem in frequency domain by

$$P_{\text{tot}} = \underbrace{\sum_{n=1}^{\infty} \iiint_{\Omega_{\text{abs}}} \frac{1}{2} \omega_n \varepsilon''(\omega_n) |\underline{\mathbf{E}}_{\text{vsr}}(\mathbf{r}, \omega_n)|^2 dV}_{P_n}, \quad (1)$$

where ω_n is the angular frequency of the n th discrete harmonic of the BESSY VSR beam current, $\varepsilon''(\omega_n)$ the imaginary part of the complex-valued permittivity at ω_n , and $\underline{\mathbf{E}}_{\text{vsr}}(\mathbf{r}, \omega_n)$ the complex-valued electric field arising from the BESSY VSR beam current at ω_n . Unfortunately, standard wakefield solvers such as included in CST Studio Suite [5] are not capable of directly determining system responses of arbitrary beam currents, particularly not of periodic beam currents. Therefore, the following workaround is used to evaluate the dissipated power (1) based on numerical computations with [5].

In a first step, the geometry under test is excited in time domain by a single Gaussian bunch carrying r.m.s. energy from $f_{\text{min}} = 0$ GHz to a finite frequency f_{max} . Often it is appropriate to introduce a small transversal offset of the beam to stimulate other modes in addition to monopole modes. The resulting transient electric fields in the absorber rings are monitored in the yz -plane with $x = 0$ mm with dedicated field probes. Note that the field probes are not directly defined on the material boundaries to avoid erroneous results. Instead, the probes are located in the vicinity of the material interfaces in the absorber ring. In a next step, the fast Fourier-transform of these transient electric fields and of the

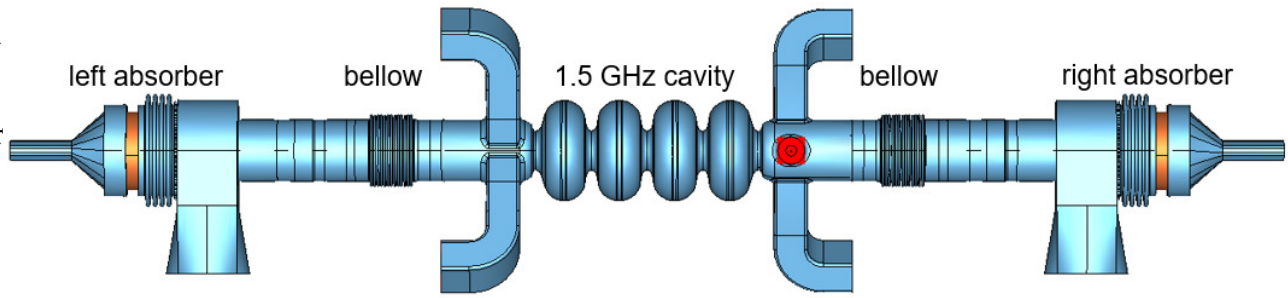


Figure 1: Simplified vacuum model of the BESSY VSR cold string with two warm end group absorbers on both sides, two bellows and one 1.5 GHz four-cell cavity used for the estimation. The vacuum is depicted in blue whereas the absorbers are indicated in orange.

current $i_{gs}(t)$ of the Gaussian bunch are computed so that a dedicated transfer function

$$\underline{\mathbf{F}}(\mathbf{r}, \omega) = \frac{\text{FFT} [\underline{\mathbf{E}}_{gs}(\mathbf{r}, t)]}{\text{FFT} [i_{gs}(t)]} \quad (2)$$

can be constructed. Based on the spatial sampling of $\underline{\mathbf{F}}(\mathbf{r}, \omega)$ in the absorber rings, the values of the transfer function are determined on the boundary of the absorbers by a 2D extrapolation using a quadratic function both for the real and the imaginary parts of $\underline{\mathbf{F}}(\mathbf{r}, \omega)$. The properties of the interpolation approach are currently under investigation. The introduced transfer function specifies the relationship of the electric fields in the lossy absorber rings and any beam current traversing the structure. In a next step, the periodic BESSY VSR beam current $i_{vsr}(t)$ (refer to Figure 2.5 in [2]) is modelled and its Fourier-transform $I_{vsr}(\omega_n)$ is determined. This allows for expressing the electric fields in the dielectric absorber rings arising from the BESSY VSR beam current spectrum by

$$\underline{\mathbf{E}}_{vsr}(\mathbf{r}, \omega_n) = \underline{\mathbf{F}}(\mathbf{r}, \omega_n) I_{vsr}(\omega_n). \quad (3)$$

The frequency samples on which the transfer function $\underline{\mathbf{F}}(\mathbf{r}, \omega)$ is available result amongst others from the resource-limited length of the wakefield run. Generally, these frequency samples do not coincide with the discrete harmonics ω_n of the BESSY VSR beam current. Thus, a spline interpolation is employed to evaluate $\underline{\mathbf{F}}(\mathbf{r}, \omega)$ on ω_n . This is appropriate since the transfer function is sufficiently smooth as a result of the absorber losses. Next, the contribution P_n of each individual harmonics to the total power P_{tot} is determined assuming that the field is of rotational symmetry:

$$P_n = \pi \omega_n \varepsilon''(\omega_n) \int_{y_{min}}^{y_{max}} \int_{z_{min}}^{z_{max}} y |\underline{\mathbf{E}}_{vsr}(0, y, z, \omega_n)|^2 dy dz. \quad (4)$$

As a matter of fact, the symmetry breaking couplers and the pump domes only slightly perturb the electric field distribution in the absorber ring. In addition, an asymmetric (i.e. an off axis) excitation of the structure slightly perturbs the symmetry of the field distribution. Formula (4) is derived under the assumption that the axes of the absorber rings are

at $x = 0$ and $y = 0$. The double integral is approximated by means of the trapezoidal rule as the electric field distribution $\underline{\mathbf{E}}_{vsr}(\mathbf{r}, \omega_n)$ is solely available at the field probes. In a final step, the power contributions of all considered harmonics are added up according to (1).

It is essential that the entire approach works with raw data delivered by the transient iteration. This allows for flexibility of the approach in terms of the software used to determine (2). Moreover, the usage of built-in Fourier transforms such as field or loss monitors in frequency domain is avoided to consistently interpret the scaling constants required for the Fourier-transforms.

NUMERICAL CALCULATIONS

To estimate the losses in the warm end groups, a simplified VSR chain composed of two bellows, one 1.5 GHz four-cell resonator, and the end groups with the dielectric absorbers (refer to Figure 1) is discretized using CST Studio Suite [5]. Obviously, less energy is deposited by the beam into the simplified string and thus into its absorber rings as only one rather than four cavities are modelled. However, introducing more cavities is connected with increasing the number of couplers which externally damp beam-excited fields. Thus, the geometry depicted in Figure 1 is considered to be a reasonable balance between the accuracy of the computational model and numerical demands such as memory requirements and computing time. The discretization of the geometry in Figure 1 resulted in approximately 960 million hexahedral mesh cells.

Based on a discrete formulation of the wave equation, the system response due the beam excitation is computed by means of the wakefield solver of [5]. The exciting Gaussian bunch has an r.m.s. length of $\sigma_{gs} = 10.5$ mm carrying r.m.s. energy up to $f_{max} = 9.752$ GHz and a small transversal offset of $\Delta x = \Delta y = 2.1$ mm to stimulate other modes in addition to monopole modes. This offset leads to a small overestimation of the losses on account of the location of the probe array (refer to the field probes marked in green in Figure 2). The frequency-dependent and complex-valued permittivity $\underline{\varepsilon}(\omega)$ of the absorber material SC-35 [6] is modelled according to measured data kindly provided by [7]. Waveguide ports are defined at both ends of the structure, at

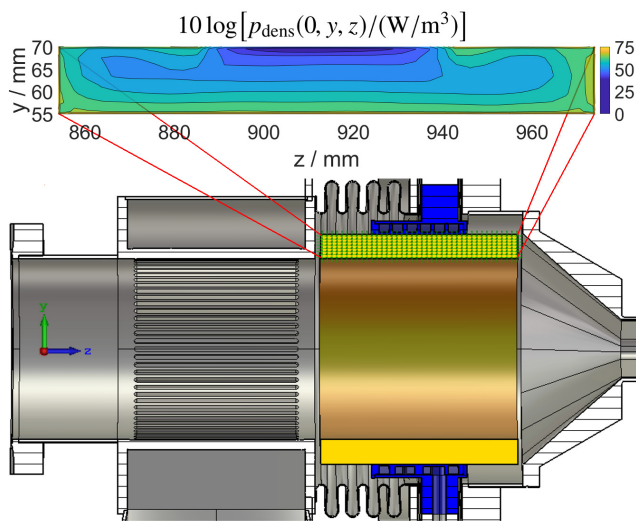


Figure 2: Cutplane (yz -plane with $x = 0$ mm) of the right end group. The dielectric absorber ring is depicted in orange and the 40×8 field probe array on which the electric field strengths are monitored is highlighted in green. A logarithmic contour plot of the power density distribution in the absorber is presented above the end group.

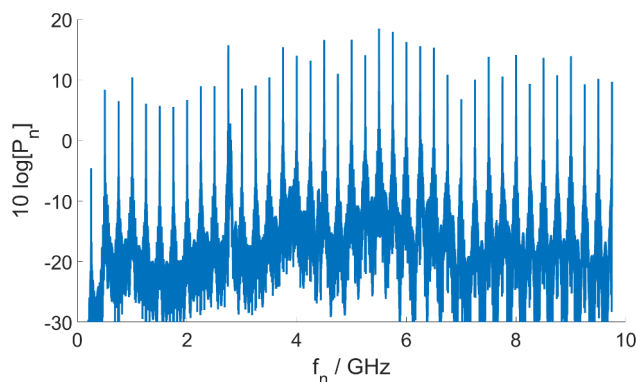


Figure 3: Logarithmic plot of spectral power components in the downstream absorber according to (4). The dominant power contributions at multiples of 250 MHz result from the BESSY VSR baseline filling pattern given in Figure 2.5 of [2].

the power coupler, and at the five higher-order mode (HOM) waveguide couplers. At each waveguide port all port modes with a cutoff frequency smaller or equal than f_{\max} are considered plus a set of evanescent port modes. This results in 15 port modes per beam pipe, 40 port modes per waveguide higher-order mode absorber, and 12 port modes for the power coupler. The simulated wavelenght is $L_{\text{wake}} = 25$ m so that the transfer function $\underline{\mathbf{F}}(\mathbf{r}, \omega)$ is sampled on the interval f_{\min} to f_{\max} with $\Delta f \approx 12$ MHz. The wakefield computation was performed on an Intel(R) Xeon(R) CPU E5-2643 v4 @ 3.40 GHz with 256 GB and required almost seven days. Figure 2 depicts the $40 \times 8 = 320$ field probes (marked in green) to monitor the electric fields in the downstream absorber ring.

Based on the introduced procedure, the losses due to the VSR baseline filling pattern with the average current of ≈ 300 mA amount to $P_{\text{tot,up}} = 788$ W in the upstream absorber and to $P_{\text{tot,down}} = 1270$ W in the downstream absorber. In the upper area of Figure 2 the corresponding power density $p_{\text{dens}}(0, y, z)$ in the downstream dielectric absorber is depicted in terms of a logarithmic contour plot. The contour plot shows that the power density resulting from dielectric losses is not homogeneously distributed across the ring. Instead, the losses are predominantly located in the vicinity of the absorber surface as the fields exponentially decay when penetrating the lossy material. Thus, it is of crucial relevance to accurately represent fields near and on the absorber surfaces. The region with comparably small loss densities at the middle top of the ring ($y \approx 70$ mm and $z \approx 890$ mm . . . 940 mm) results from the cooling jacket (depicted in blue in the end group shown in Figure 2) of the absorber which acts as an electromagnetic shield.

Figure 3 depicts the spectral components contributing to the total power P_{tot} in the downstream absorber. The diagram shows that P_n does not drop at higher frequencies so that higher harmonics beyond the considered $f_{\max} = 9.752$ GHz contribute to the overall power according to (1) as well. Tests with a further simplified structure solely consisting of the end groups showed that P_n becomes negligible only for frequencies larger than 20 GHz.

DISCUSSION AND OUTLOOK

The computed loss values P_{tot} are in the order of the expectation. However, the presented loss values are significantly higher than the loss values provided in [8]. The smaller loss values in [8] are attributed to a coarser sampling of the fields in the absorber using probes (particularly in the vicinity of the material interfaces) and to not using an extrapolation approach. Studies have shown that the location of the field probes strongly influences the total losses on account of the inhomogeneous power density distributions in the ring. Thus, additional studies are required, e.g. on the interpolation approach. Furthermore, uncertainties arise from the simplification of the string, the assumption of symmetry (despite the fact that the structure and the excitation is slightly asymmetric), and the restriction to $f_{\max} = 9.752$ GHz.

Nonetheless, thermal simulations are in preparation to determine the temperature distribution in the absorber rings. The power density distribution at the top of Figure 2 multiplied with a contingency factor of two serves as driving source for the thermal simulations. Amongst others, the contingency factor results from studies with the aforementioned further simplified structure solely consisting of the end groups. On account of the small thermal conductivity of the dielectric absorbers, large temperature gradients can arise on the surfaces from the inhomogeneous distribution of the power density. Large temperature gradients can be critical for brittle ceramics.

ACKNOWLEDGEMENT

The authors would like to thank Frank Marhauser from Jefferson National Laboratory for kindly providing tables with measured frequency-dependent material parameters of the dielectric absorber rings and for carefully reading and improving the manuscript.

Furthermore, the authors are grateful to Felix Glöckner and Marc Dirsat from Helmholtz-Zentrum Berlin for various discussions on mechanical properties of dielectric absorbers and for currently preparing the thermal simulations.

REFERENCES

- [1] G. Wüstefeld, A. Jankowiak, J. Knobloch, and M. Ries, “Simultaneous Long and Short Electron Bunches in the BESSY II Storage Ring”, IPAC 2011, San Sebastián, Spain, 2011.
- [2] A. Jankowiak et al., “Technical Design Study BESSY VSR”, Helmholtz-Zentrum Berlin, Berlin, Germany, 2015.
- [3] A. Vélez et al., “The SRF Module Developments for BESSY VSR”, IPAC 2017, Copenhagen, Denmark, 2017.
- [4] A. Tsakanian et al., “Study on HOM Power Levels in the BESSY VSR Module”, IPAC 2017, Copenhagen, Denmark, 2017.
- [5] CST Studio Suite 2017 is available from CST GmbH, Bad Nauheimer Str. 19, 64289 Darmstadt, Germany.
- [6] CoorsTek Inc., 14143 Denver West Pkwy., Golden, CO 80401, USA.
- [7] F. Marhauser from Jefferson National Laboratory, private communication, 2017.
- [8] A. Tsakanian et al., “HOM Power Levels in the BESSY VSR Cold String”, IPAC 2018, Vancouver, Canada, 2018.